PERGAMON

International Journal of Heat and Mass Transfer 43 (2000) 3755–3764

International Journal of HEAT and MASS TRANSFER

www.elsevier.com/locate/ijhmt

# A study of multiple heat sources on a flat plate heat pipe using a point source approach

B.K. Tan, X.Y. Huang, T.N. Wong*, K.T. Ooi

*School of Mechanical and Production Engineering, Nanyang Technological University, Nanyang Avenue, Singapore 639798*

Received 7 May 1999; received in revised form 7 January 2000

**Abstract**

An analytical approach has been employed to study liquid flows in an isotropic wick structure of a flat plate heat pipe with multiple heat sources. In this study, the heat sources have been modeled as point sources using the Dirac Delta function to describe the heat distribution. The two-dimensional pressure and velocity distributions are shown and discussed. The study has been extended to locate the positions of the multiple heat sources for optimum heat pipe performance. The optimum performance of the heat pipe is accomplished when the minimum pressure drop is attained across the wick structure. 

## 1. Introduction

The integration and miniaturization of modern electronic systems have resulted in higher heat fluxes generated at the chip and module level of the system. Therefore, effective cooling devices are needed to keep the systems operating at their reliable working temperature levels. Heat pipes have been widely used in the thermal management of electronic systems. Their ability to transport heat over a substantial distance at low temperature drops has made them a much reliable and efficient cooling device.

It is commonly predicted that the electronic systems in the next generation will be more compact and smaller in size. Thus, more integrated circuits chips (IC) will be incorporated into a single printed circuit board (PCB) and inevitably generating more high temperature spots at the board level. In order to overcome the high heat dissipation requirement, a passive device such as heat pipe may be used to cool the system under multiple source heating condition. Hence, it is timely to evaluate the performance of the heat pipe under such condition. In this case, locations of the heat sources that allow optimum performance of the heat pipe must be sought for.

The variations of the pressure distribution for both the vapor core and wick structure of a heat pipe affect significantly the capillary limit or optimum operating performance of the device [1]. For example, the analysis of the liquid flow field under circumferential heating mode, i.e. when the heat source covers the entire heat pipe's evaporation, is quite different from that of the block-heating mode. This is because the liquid flow in the wick structure is no longer one-dimensional. When the heater covers partially on the heat pipe surface, there exists transverse velocity components and the liquid flow field becomes two-dimensional instead.

Investigations of the heat pipe under circumferential and block-heating conditions were carried out during the past decade. Both Schmalhofer and Faghri [2] had carried out experimental and analyti-

* Corresponding author. Tel.: +65-799-5587; fax: +65-791-1859.

*E-mail address:* mtnwong@ntu.edu.sg (T.N. Wong).

0017-9310/00/$ - see front matter 
PII: S0017-9310(00)00016-8

**Nomenclature**

| | |
|---|---|
| $a$ | length of the flat plate heat pipe (m) |
| $A_{mn}$ | Fourier coefficients of $p$ |
| $b$ | width of the flat plate heat pipe (m) |
| $d$ | distance between two-point heat sources (m) |
| $f(x, y)$ | distribution function of the condensation rate |
| $F_{mn}$ | Fourier coefficients of $f(x, y)$ |
| $K$ | wick permeability |
| $p$ | pressure (Pa) |
| $p_{\text{ref}}$ | reference pressure (Pa) |
| $P$ | non-dimensional pressure |
| $x_0, y_0$ | $x$ and $y$ coordinates of the point source (m) |
| $u, v$ | velocity components in the $x$ and $y$ direction (m $s^{-1}$) |
| $U, V$ | non-dimensional velocity components in the $x$ and $y$ direction |
| $x, y$ | axial and transverse coordinates (m) |
| $X, Y$ | non-dimensional axial and transverse coordinates |

*Greek symbols*

| | |
|---|---|
| $\alpha$ | general condensation rate in the wick structure (kg $s^{-1}$ $m^{-2}$) |
| $\alpha^+$ | condensation rate (kg $s^{-1}$ $m^{-2}$) |
| $\alpha^-$ | evaporation rate (kg $s^{-1}$ $m^{-2}$) |
| $\beta$ | $= \mu\alpha^+/\rho K$ (kg $s^{-2}$ $m^{-3}$) |
| $\eta$ | ratio of the condensation area to evaporation area |
| $\mu$ | dynamic viscosity of liquid (N s $m^{-2}$) |
| $\rho$ | surface density of liquid (kg $m^{-2}$) |

cal works on the circular heat pipe under circumferental and block heating modes. In addition, Huang and Liu [3] presented an analytical model to calculate the liquid pressure and velocity distributions in the isotropic wick structure of a flat plate heat pipe under localized heating condition where a heater was fixed at the end of the heat pipe. More recently, Qin and Liu [4] reported an analytical solution of liquid flow in the anisotropic permeability wick of a flat plate heat pipe. It was found that the anisotropic wick property and the heater location affect significantly the overall pressure and velocity distributions of the working fluid inside the heat pipe.

For heat pipes with multiple heat sources, Fahgri and Buchko [5] carried out both the experimental and the numerical analysis for circular heat pipes operating at low temperatures. In their work, it was concluded that the maximum heat load on the heat pipe varied greatly with the locations of the local heat fluxes.

An analytical evaluation on the liquid pressure and velocity distributions of a flat plate heat pipe with multiple heat sources is presented in this paper. The heat sources are simulated as point source by employing the Dirac Delta function. This approach helps to formulate the source distribution function of the condensation rate during the analysis. It is advantageous to consider the heat input zone as a point source because it simplifies the analysis and yet provides good qualitative accounts on actual heat transfer on the heat pipe surface.

As the heat sources' locations on the heat pipe are important for an optimum heat pipe performance, it is more appropriate to position the high temperature chips at their optimum locations where the heat pipe can further dissipate the heat efficiently. The formulated analytical model, which is solved using double Fourier series expansion method, is capable of optimizing the point source positions on a flat plate heat pipe under multiple source heating condition. In this paper, the application of point heat source will be shown and the optimized positions of one-, two- and four-point heat sources on a flat plate heat pipe will be discussed.

## 2. Formulation and solution

The liquid pressure and velocity fields in the isotropic wick structure are evaluated analytically by considering a single point heat source placed on the flat plate heat pipe. Using this analysis, the formulation is then extended to solve the liquid pressure and velocity fields when two- and four-point heat sources are placed on the heat pipe.

As illustrated in Fig. 1, the flat plate heat pipe is of $a \times b$ dimension and the single point heat source is arbitrarily located at $(x_0, y_0)$ on the heat pipe surface. The working fluid inside the heat pipe is assumed to be evaporated uniformly over the heat source at an evaporation rate of $\alpha^-$ (kg $s^{-1}$ $m^{-2}$). For the heat pipe's surface outside the heat source, the vapor is to be condensed uniformly into the wick at a condensation rate of $\alpha^+$ (kg $s^{-1}$ $m^{-2}$).

The working fluid evaporated from the point heat source is considered to be condensed back into the fluid at a negative condensation rate of $-\alpha^- = -\eta\alpha^+$, where $\eta$ is a constant. Thus, the condensation rate over the entire heat pipe surface can be expressed as:

$$\alpha = \alpha^+ f(x, y) \tag{1}$$

where $f(x, y)$ is the distribution function of the condensation rate and it can then be written as follows:

$$f(x,y) = \begin{cases} 1, & (x,y) \in S \\ -\eta, & (x,y) \in R \end{cases} \tag{2}$$

with $S$ and $R$ being referred to as the condensation and evaporation zone, respectively. In addition, if adiabatic sections are to be included in the analysis, the distribution function $f(x, y)$ will be zero inside the adiabatic boundary.

The dimensional ratio of the condensation and evaporation rate, η, can be evaluated by considering the mass conversation, i.e.,

$$\int\int_s f(x,y)\,\mathrm{d}x\,\mathrm{d}y = 0 \tag{3}$$

In this model using a point heat source, Dirac Delta function is used to express the overall distribution function of the condensation rate, $f(x, y)$. Hence, the distribution function $f(x, y)$ with a point heat source located at $(x_0, y_0)$ on the heat pipe surface can be expressed as:

$$f(x,y) = 1 - \eta\delta(x - x_0)\delta(y - y_0) \tag{4}$$

The dimensional ratio of the condensation and evaporation rate, η, can then be evaluated using Eqs. (3) and (4), and hence, for a single point heat source,

$$\eta = ab \tag{5}$$

The working fluid is in a porous material and it is assumed to follow Darcy's law. The governing equations for the liquid flow in the wick structure can be written as:

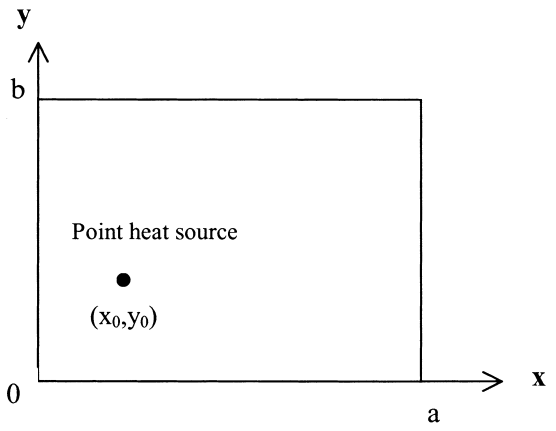


Fig. 1. An illustration of the flat plate heat pipe with an arbitrary placed point heat source.

$$u = -\frac{K}{\mu}\frac{\partial p}{\partial x}; \quad v = -\frac{K}{\mu}\frac{\partial p}{\partial y} \tag{6}$$

$$\frac{\partial u}{\partial x} + \frac{\partial v}{\partial y} = \frac{\alpha}{\rho} \tag{7}$$

where $p$ is the pressure of the liquid, $u$ and $v$ are the flow velocities in the $x$ and $y$ direction, respectively. $K$ is the wick permeability of the wick structure, α is the general condensation rate while $\mu$ and $\rho$ are the dynamic viscosity and surface density of the working fluid, respectively.

By combining Eqs. (6) and (7), together with Eq. (1), it yields an expression for the pressure $p$ as such:

$$\frac{\partial^2 p}{\partial x^2} + \frac{\partial^2 p}{\partial y^2} = -\beta f(x,y) \tag{8}$$

where $\beta = \frac{\mu\alpha^+}{\rho K}$. Due to the zero flow velocity at the boundaries, the boundary conditions for the pressure are:

$$\left.\frac{\partial p}{\partial x}\right|_{x=0} = \left.\frac{\partial p}{\partial x}\right|_{x=a} = \left.\frac{\partial p}{\partial y}\right|_{y=0} = \left.\frac{\partial p}{\partial y}\right|_{y=b} = 0 \tag{9}$$

Following the technique presented by Huang and Liu [3], the pressure distribution can be expanded in the form of a double Fourier series shown as follows:

$$p = p_{\mathrm{ref}} + \beta ab\left\{\sum_{m=1}^{\infty} A_{m0}\cos\frac{m\pi x}{a} + \sum_{n=1}^{\infty} A_{0n}\cos\frac{n\pi y}{b} + \sum_{m=1}^{\infty}\sum_{n=1}^{\infty} A_{mn}\cos\frac{m\pi x}{a}\cos\frac{n\pi y}{b}\right\} \tag{10}$$

In the above equation, $p_{\mathrm{ref}}$ is the reference pressure of the working fluid and the Fourier coefficients of $A_{mn}$ can be determined by substituting Eq. (10) into Eq. (8), which gives,

$$ab\left\{\sum_{m=1}^{\infty} A_{m0}\left(\frac{m\pi}{a}\right)^2\cos\frac{m\pi x}{a} + \sum_{n=1}^{\infty} A_{0n}\left(\frac{n\pi}{b}\right)^2\cos\frac{n\pi y}{b} + \sum_{m=1}^{\infty}\sum_{n=1}^{\infty} A_{mn}\left[\left(\frac{m\pi}{a}\right)^2 + \left(\frac{n\pi}{b}\right)^2\right]\cos\frac{m\pi x}{a}\cos\frac{n\pi y}{b}\right\} = f(x,y) \tag{11}$$

The distribution function $f(x, y)$ can also be expressed as in the same Fourier's series,

$$f(x,y)=\sum_{m=1}^{\infty}F_{m0}\cos\frac{m\pi x}{a}+\sum_{n=1}^{\infty}F_{0n}\cos\frac{n\pi y}{b}+\sum_{m=1}^{\infty}\sum_{n=1}^{\infty}F_{mn}\cos\frac{m\pi x}{a}\cos\frac{n\pi y}{b} \tag{12}$$

where $F_{m0}=-\eta\cos\frac{m\pi x_0}{a}$, $F_{0n}=-\eta\cos\frac{n\pi x_0}{b}$, $F_{mn}=-\eta\cos\frac{m\pi x_0}{a}\cos\frac{n\pi y_0}{b}$.

Hence, by substituting Eq. (12) into Eq. (11) and comparing the coefficients of both sides, the coefficients $A_{mn}$ are found to be:

$$A_{m0}=\frac{2}{b^2(m\pi)^2}F_{m0}=\frac{-2a}{b(m\pi)^2}\cos\frac{m\pi x_0}{a} \tag{13a}$$

$$A_{0n}=\frac{2}{a^2(n\pi)^2}F_{mn}=\frac{-2b}{a(n\pi)^2}\cos\frac{n\pi y_0}{b} \tag{13b}$$

$$A_{mn}=\frac{4}{b^2(m\pi)^2+a^2(n\pi)^2}F_{mn}=\frac{-4ab}{b^2(m\pi)^2+a^2(n\pi)^2}\cos\frac{m\pi x_0}{a}\cos\frac{n\pi y_0}{b} \tag{13c}$$

Next, by setting the following parameters into the various normalized forms,

$$P=\frac{p-P_{\mathrm{ref}}}{\beta ab},\quad U=\frac{u}{\alpha^{+}b/\rho},\quad V=\frac{v}{\alpha^{+}b/\rho},\quad X=\frac{x}{a},\quad Y=\frac{y}{b}$$

the analytical liquid pressure and velocity fields in the isotropic wick structure under a point heat source heating condition can be expressed as such:

$$P=\sum_{m=1}^{\infty}A_{m0}\cos(m\pi X)+\sum_{n=1}^{\infty}A_{0n}\cos(n\pi Y)+\sum_{m=1}^{\infty}\sum_{n=1}^{\infty}A_{mn}\cos(m\pi X)\cos(n\pi Y) \tag{14}$$

$$U=-\frac{\partial P}{\partial X}=\sum_{m=1}^{\infty}A_{m0}(m\pi)\sin(m\pi X)+\sum_{m=1}^{\infty}\sum_{n=1}^{\infty}A_{mn}(m\pi)\sin(m\pi X)\cos(n\pi Y) \tag{15}$$

$$V=-\frac{a}{b}\frac{\partial P}{\partial Y}=\frac{a}{b}\left\{\sum_{n=1}^{\infty}A_{0n}(n\pi)\sin(n\pi Y)+\sum_{m=1}^{\infty}\sum_{n=1}^{\infty}A_{mn}(n\pi)\cos(m\pi X)\sin(n\pi Y)\right\} \tag{16}$$

Similarly, if the heat pipe is subjected to two-point heat sources located at $(x_0,y_0)$ and $(x_1,y_1)$ with the same heat strength, the distribution function can be expressed as:

$$f(x,y)=1-\frac{\eta}{2}\delta(x-x_0)\delta(y-y_0)-\frac{\eta}{2}\delta(x-x_1)\delta(y-y_1) \tag{17}$$

If four-point heat sources are placed on the heat pipe surface, the distribution function can be related as:

$$f(x,y)=1-\frac{\eta}{4}\delta(x-x_0)\delta(y-y_0)-\frac{\eta}{4}\delta(x-x_1)\delta(y-y_1)-\frac{\eta}{4}\delta(x-x_2)\delta(y-y_2)-\frac{\eta}{4}\delta(x-x_3)\delta(y-y_3) \tag{18}$$

Hence, by using the Delta function, the distribution function $f(x,y)$ can be developed to express the distribution of any number of point heat sources on the heat pipe surface. Using Eqs. (14)–(16), the pressure and velocity distribution can be calculated analytically. Results of using a one-, two- and four-point heat sources on the flat plate heat pipe will be presented and discussed in the next section.

## 3. Results and discussion

The pressure and velocity distributions of one-, two- and four-point heat sources are evaluated and presented in this section. In addition, the various optimized locations of the point heat sources will be determined based on the results from the liquid pressure difference in the wick structure.

In the analytical model, the point heat sources with constant heat input are arbitrarily placed on the heat pipe surface. The infinite series employed in the analytical solutions are truncated at $m=n=40$, where further increments in the number of Fourier terms will have insignificant improvement in the accuracy. The pressure fields are shown by contours with non-dimensional pressure difference, $\Delta P(X,\ Y)=(P-P_{\min})/(P_{\max}-P_{\min})$, where $P_{\min}$ and $P_{\max}$ are the non-dimensional minimum and maximum pressures in the wick structure, respectively. Meanwhile, the velocity fields are represented with in the vector form,

$\vec{V} = Ui + Vj$, with $i$ and $j$ being units vectors in the $x$ and $y$ directions, respectively.

Figs. 2a and b illustrate the analytical pressure and velocity distributions of a point heat source when it was positioned at $x/a = y/b = 0.3$, a location on the diagonal axis of the heat pipe surface. It is observed from Fig. 2 that the minimum pressure is always at the heat source region, while the maximum pressure is found at localities further from the heat source. It was noted that at this position, the maximum liquid pressure difference across the wick structure is $\Delta P_{max} = 0.735$ at $x/a = y/b = 1$. In Fig. 2b, it is seen that the working liquid is flowing back to the point heat source position from all directions.

For the single point heat source on the heat pipe surface, the optimized position was found to be at the center position of the heat pipe surface. From the illustration in Fig. 3, minimum point was determined at $x/a = 0.5$ for both cases when the point heat source lies on both the diagonal and the horizontal axis ($y/a = 0.5$) of the heat pipe surface. At this position, the liquid pressure difference in the wick structure pipe is the lowest, indicating the heat pipe is operating at its optimum capacity. This result agrees with that of Huang and Liu [3] where the best position to place a strip heater is at the center of the flat plate heat pipe. The pressure and velocity distributions of the optimized position of a single point heat source are shown in Figs. 4a and b. Notice that at this optimum position, the maximum liquid pressure difference ($\Delta P_{max} =$ 0.623 at all four corner positions) is the lowest compared to the other locations as discussed in Fig. 3.

Instead of a single heat source condition on a conventional heat pipe operation, optimization of multiple source heating condition on a flat plate heat pipe was carried out, which may resolve the multiple hot spots heating on a PCB. When two-point heat sources or more are placed on the heat pipe, the optimized position is no longer at the center of the heat pipe. Figs. 5a and b represent the plots of the optimized location of two point sources when they are positioned along the diagonal and the horizontal axis ($y/b = 0.5$), respectively. Distance $d$ is introduced for both cases, which describe the distance between the two-point sources with reference to the center (i.e. $x/a = y/b = 0.5$) of the heat pipe, respectively. It is observed from both cases that when the distances $d$ are small, i.e. the two heat sources are placed close to one another near the center of the heat pipe, the maximum 1iquid pressure difference is the highest. Minimum points are determined on the plots that indicate the optimized positions of the two-point heat sources on the heat pipe surface. In these optimized positions, minimal liquid pressure drop is attained.

From Fig. 5a, when both the two-point heat sources are $d/a = 0.424$ apart along the diagonal axis, its liquid pressure drop is the lowest and optimized positions were achieved. Similarly, in Fig. 5b, when two-point sources are placed along the horizontal axis, the optimized positions are found when they are at a distance

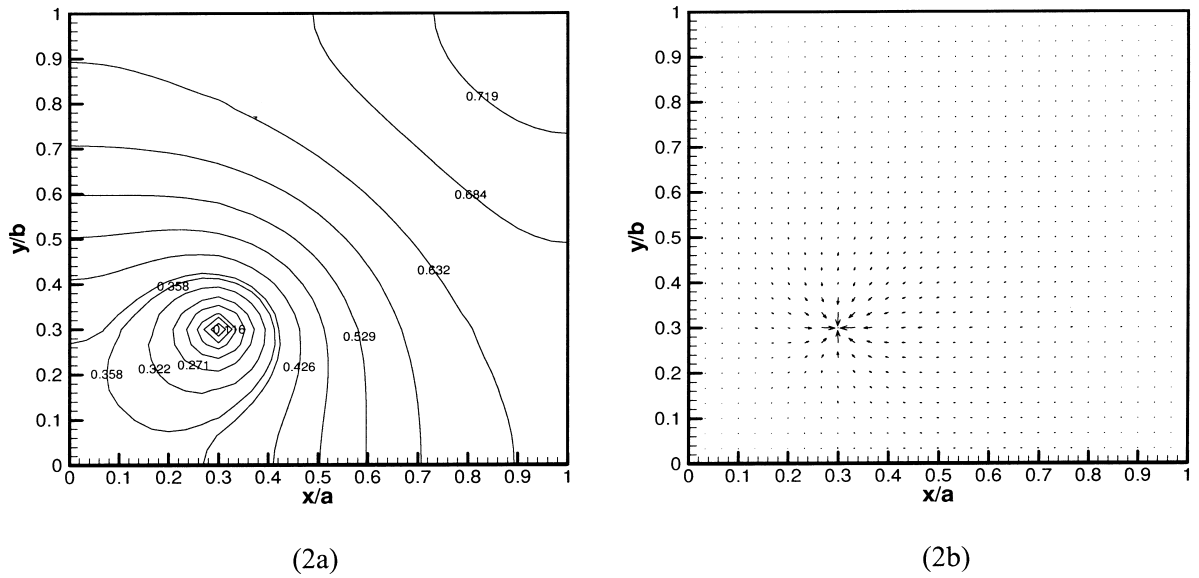


Fig. 2. Pressure (a) and velocity (b) distributions of a point source when $x/a = y/b = 0.3$.

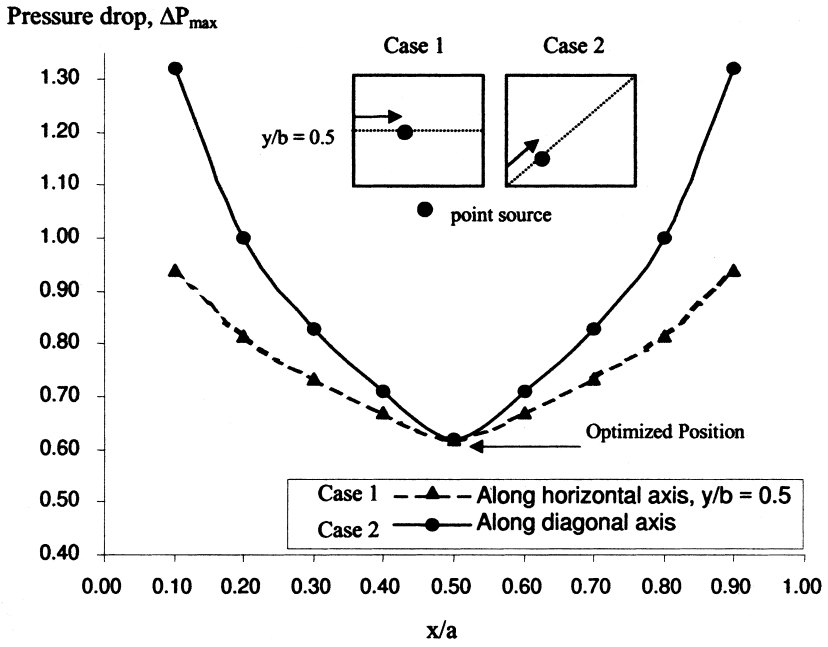


Fig. 3. Maximum liquid pressure drop versus the location of a point heat source on the heat pipe surface. Case 1: point source lies along the horizontal axis, $y/b = 0.5$. Case 2: point source lies along the diagonal axis.

of $d/a = 0.5$ apart on the heat pipe's surface with reference to the center of the heat pipe. The liquid pressure and velocity distribution plots of the optimized positions of the two-point sources on the horizontal axis is presented in Figs. 6a and b, respectively. It is seen that the pressure contours and velocity vectors near both the heat sources are similar and symmetrical in their distribution. While in Fig. 6a, the liquid pressure drop across the wick structure is $\Delta P_{\max} = 0.309$ at $x/a = y/b = 1$. This value is the least

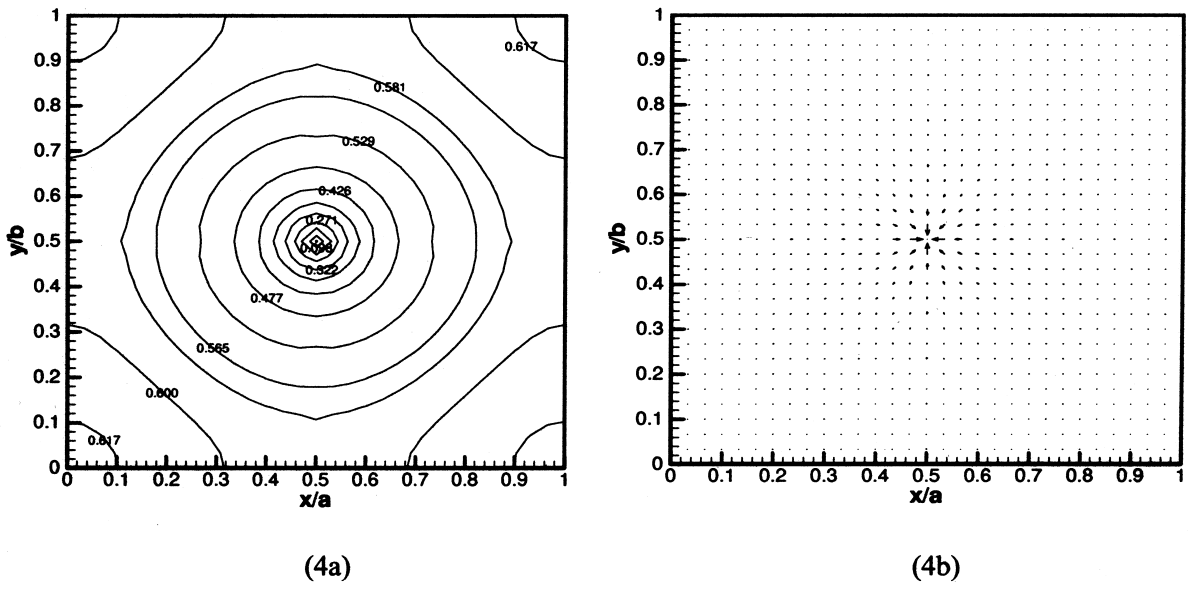


Fig. 4. Pressure (a) and velocity (b) distributions of the optimized position of a point source when $x/a = y/b = 0.5$.

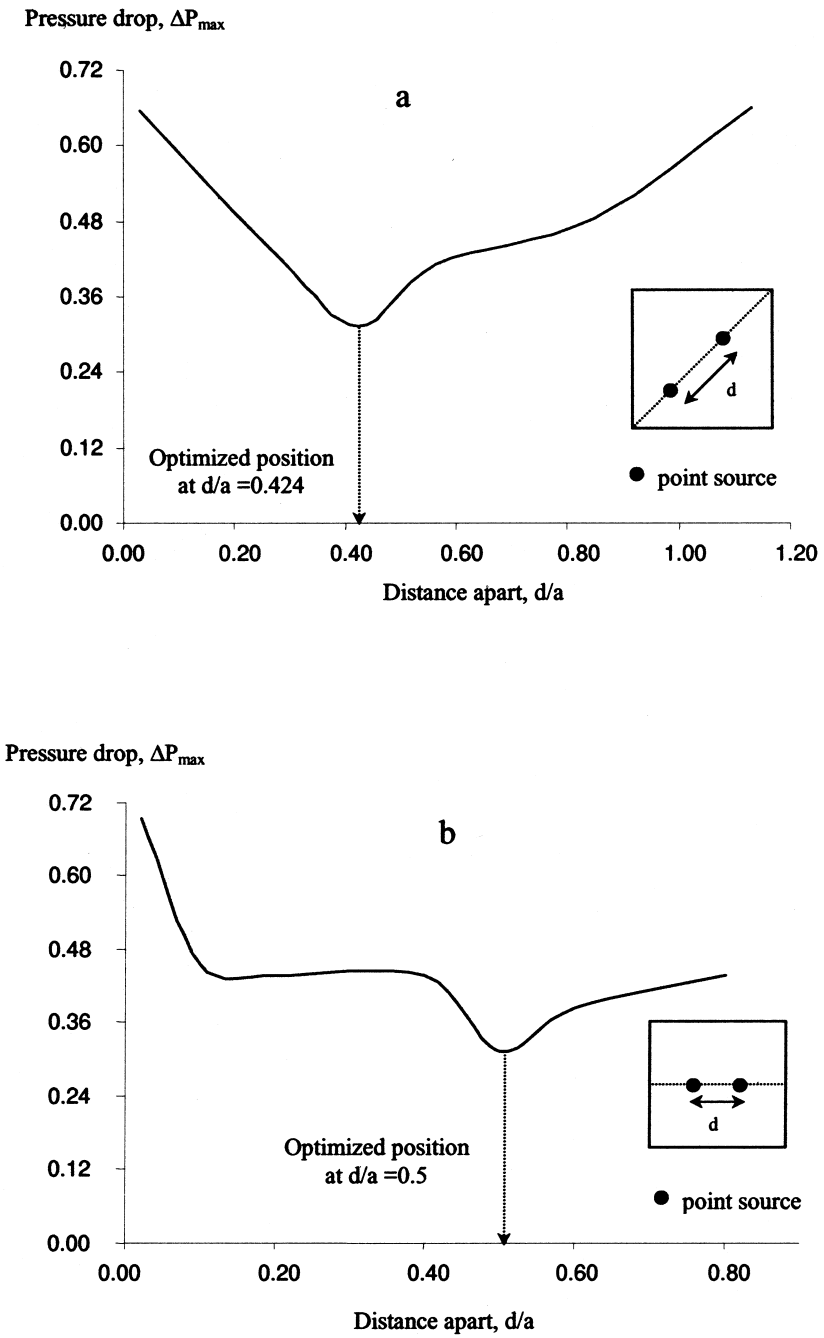


Fig. 5. (a) Maximum liquid pressure drop versus the location of two-point heat sources when they are varied along the diagonal axis of the heat pipe. (b) Maximum liquid pressure drop versus the location of two point heat sources when they are varied along the horizontal axis ($y/b = 0.5$) of the heat pipe.

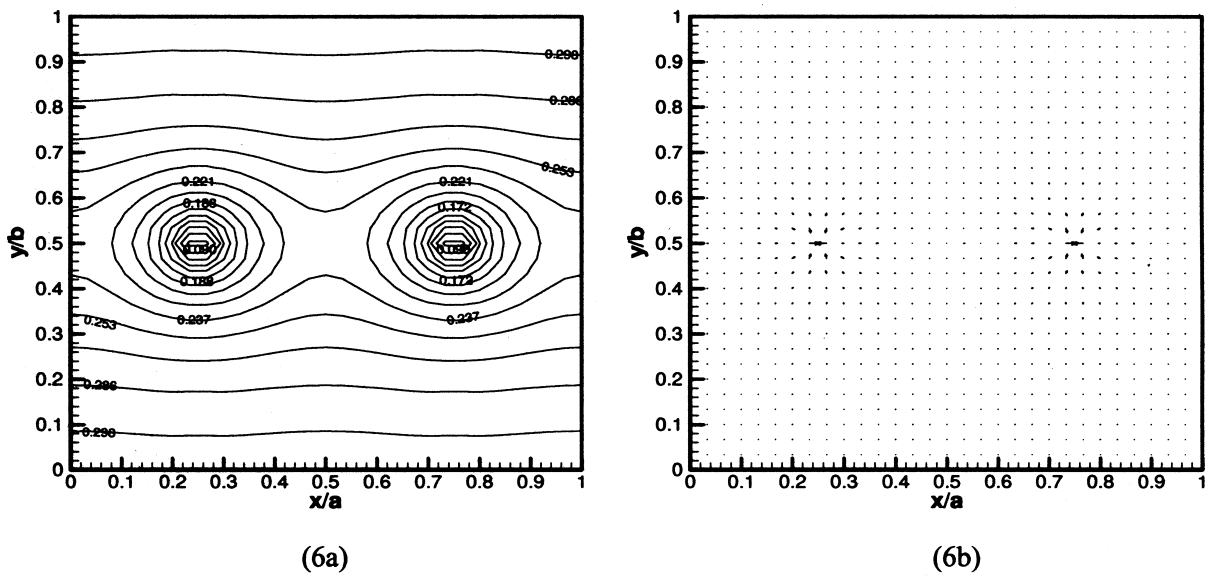


Fig. 6. The pressure (a) and velocity (b) distributions of the optimized positions of two-point heat sources on the horizontal axis.

as compared to the values of other arrangements shown in Fig. 5b.

The optimization of the four-point heat source locations is also determined. Fig. 7 relates the variation of the maximum liquid pressure difference when the four-point heat sources are varied along the two diagonals of the heat pipe surface. It was found that the optimized positions of these four-point heat sources are located when they are placed at a distance $d/a = 0.707$ apart on the diagonals with reference to the cen-

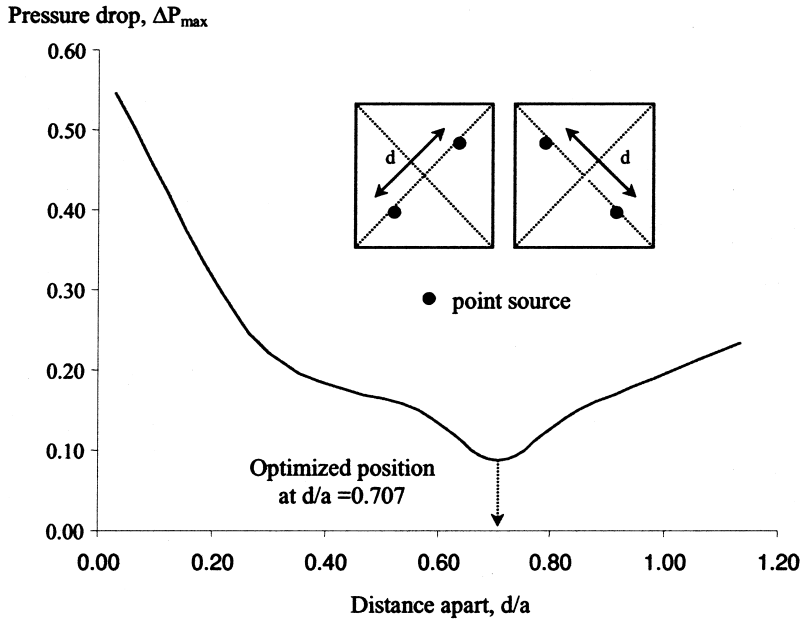


Fig. 7. Maximum liquid pressure drop versus the location of four-point heat sources when they are varied along the diagonal axis of the heat pipe.

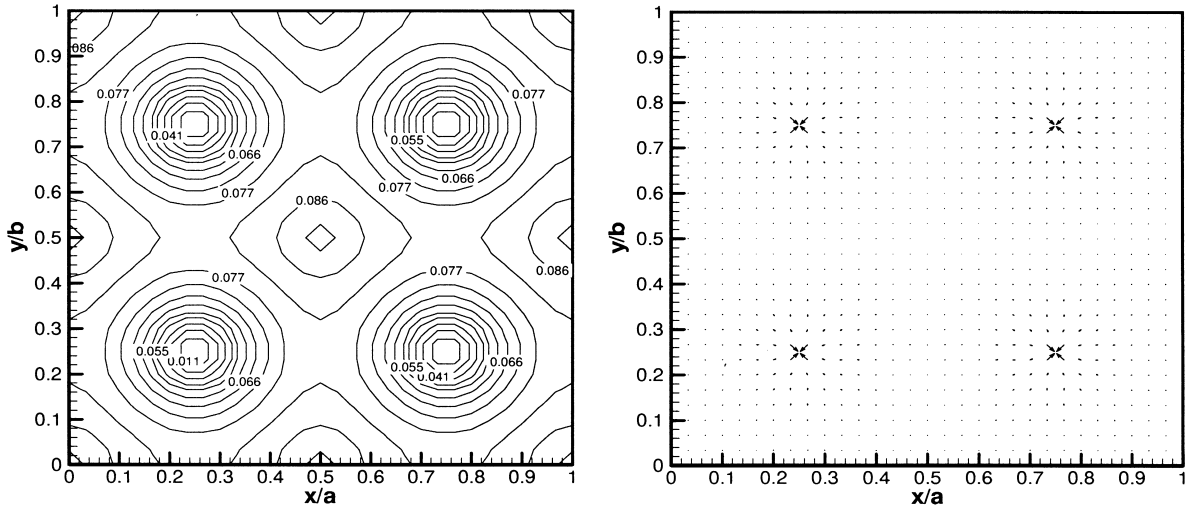


Fig. 8. The pressure (a) and velocity (b) vector plots of the optimized positions of four-point heat sources on the diagonal axis.

ter of the heat pipe. Symmetrical distribution features were also observed in Figs. 8a and b which clearly illustrate the pressure and velocity contours of the optimized positions when the four-point heat sources are positioned at the two diagonal axes.

These optimized positions can be justified by considering the derivative of the liquid pressure (Eq. (14)) with respect to the distance $d$. Fig. 9 illustrates a relation of $\partial P/\partial d$ and $d/a$ when the two-point heat sources are varied along the horizontal axis on the heat pipe surface. It shows that $\partial P/\partial d$ changes from positive to negative, though a fluctuation is observed which may probably be attributed to the truncation of $\partial P/\partial d$. It is shown that minimum point occurs at

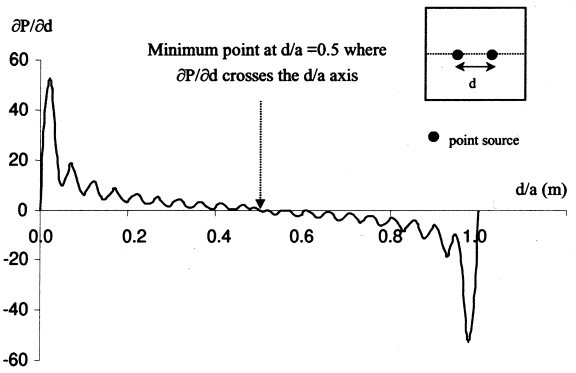


Fig. 9. The derivative of the liquid's pressure with respect to the horizontal distance apart, $d/a$ so as to verify the optimum positions of the two-point heat sources.

$d/a = 0.5$ when $\partial P/\partial d = 0$. Hence, it is obvious that at $d/a = 0.5$, the two optimized heat sources' positions are located at $x_0/a = 0.25$ and $x_1/a = 0.75$ on the heat pipe surface which agree with what was presented in Fig. 5b. Therefore, the other optimized positions can also be verified by considering this derivative method of the liquid pressure in the wick structure.

Optimization of the point heat source locations can be achieved using this analytical model. When the heat sources are placed arbitrarily on the heat pipe, maximum capillary limit may not be achieved, and hence, the heat pipe will be under utilized. Henceforth, by positioning any number of the point heat sources at their optimized locations, the heat pipe will still cool the hot spots effectively while achieving its maximum capillary limit.

## 4. Concluding remarks

The simplified analytical model employing point source is capable of predicting qualitatively the pressure and velocity distributions in a two-dimensional flat plate heat pipe. The analysis is particularly suitable for locating heat source positions for optimum heat pipe performance. The results show that, for a single point heat source, the optimized location is at the center of the heat pipe as expected. While for the case of two- and four-point heat sources, optimized positions can be achieved when the heat sources are placed symmetrically to one another with respect to the center of the heat pipe. At these optimized locations, minimal

liquid pressure drop is achieved across the wick structure in the heat pipe as compared to the other heat sources' positions. In this case, the heat pipe is said to have achieved its maximum capillary limit. It is believed that the analysis is best suited if the PCB and different capacity of heat sources are presented on a design.

## References

[1] P.D. Dunn, D.A. Reay, Heat Pipes, 4th ed., Pergamon Press, Oxford, 1994.
[2] J. Schmalfoher, A. Fahgri, A study of circumferential heated and block heated heat pipes—I. Experimental analysis and generalized analytical prediction of capillary limits, Int. J. Heat Mass Transfer 36 (1) (1993) 201–212.
[3] X.Y. Huang, C.Y. Liu, The pressure and velocity fields in the wick structure of a localized heated flat plate heat pipe, Int. J. Heat Mass Transfer 39 (6) (1996) 1325–1330.
[4] W. Qin, C.Y Liu, Liquid flow in the anisotropic wick structure of a flat plate heat pipe under block heating condition, Applied Thermal Engineering 17 (4) (1997) 339–349.
[5] A. Faghri, M. Buchko, Experimental and numerical analysis of low temperature heat pipes with multiple heat sources, ASME Journal of Heat Transfer 113 (1991) 728–734.